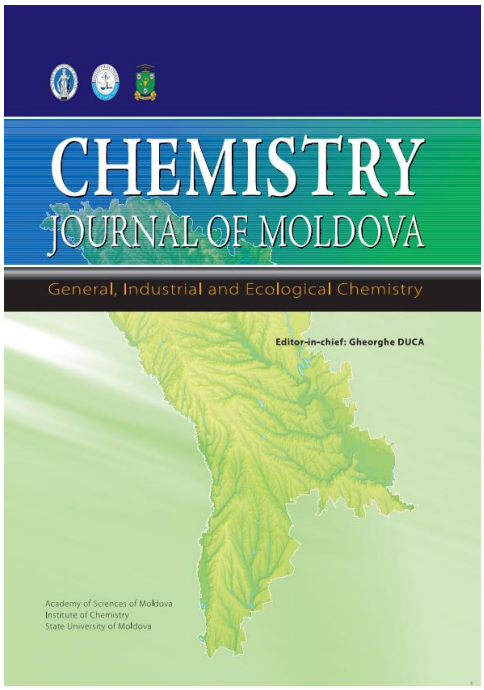

CHEMISTRY JOURNAL OF MOLDOVA.
General, Industrial and Ecological Chemistry

Publication details, including instructions for authors information:
http://cjm.ichem.md/

IMIDAZOLE-FUNCTIONALIZED PYRIDINIUM-FUSED SELENADIAZOLIUM SALTS AS VERSATILE CHALCOGEN BOND DONORS

Evgeny Dukhnovsky[a], Namiq Shikhaliyev[b*], Alexander Sapronov[a], Alexey Kubasov[c], Alexander Novikov[d], Alexander Tskhovrebov[a], Gulnaz Mirzayeva[e]

[a]*Peoples' Friendship University of Russia, 6, Miklukho-Maklaya str., Moscow, Russia*
[b]*Department of Chemical Engineering, Baku Engineering University, 120 Hasan Aliyev str., Baku, AZ0101, Azerbaijan*
[c]*Kurnakov Institute of General and Inorganic Chemistry, Russian Academy of Sciences, 31, Leninsky prosp., Moscow, Russia*
[d]*Institute of Chemistry, Saint Petersburg State University, 7/9, Universitetskaya nab., Saint Petersburg, Russia*
[e]*Department of Chemical Technology, Recycling and Ecology, Azerbaijan Technical University, 25, H.Javid ave, Baku, Azerbaijan*
[*]*e-mail: namiqst@gmail.com, +994503225269*

Accepted version posted online: 15 June 2026

To cite this article: E. Dukhnovsky, N. Shikhaliyev, A. Sapronov, A. Kubasov, A. Novikov, A. Tskhovrebov, G. Mirzayeva. Imidazole-Functionalized Pyridinium-Fused Selenadiazolium Salts as Versatile Chalcogen Bond Donors. *Chemistry Journal of Moldova*, *2026*, DOI: doi.org/10.19261/cjm.2026.1478

CHEMISTRY JOURNAL OF MOLDOVA. General, Industrial and Ecological Chemistry
ISSN (p) 1857-1727 ISSN (e) 2345-1688
http://cjm.ichem.md
https://doi.org/10.19261/cjm.2026.1478

IMIDAZOLE-FUNCTIONALIZED PYRIDINIUM-FUSED SELENADIAZOLIUM SALTS AS VERSATILE CHALCOGEN BOND DONORS

Evgeny Dukhnovsky [a], Namiq Shikhaliyev [b*], Alexander Sapronov [a], Alexey Kubasov [c], Alexander Novikov [d], Alexander Tskhovrebov [a], Gulnaz Mirzayeva [e]

[a]*Peoples' Friendship University of Russia, 6 Miklukho-Maklaya str., Moscow, Russia*
[b]*Department of Chemical Engineering, Baku Engineering University,120 Hasan Aliyev str., Baku, AZ0101, Azerbaijan*
[c]*Kurnakov Institute of General and Inorganic Chemistry, Russian Academy of Sciences, 31, Leninsky prosp., Moscow, Russia*
[d]*Institute of Chemistry, Saint Petersburg State University, 7/9, Universitetskaya Nab., Saint Petersburg, Russia*
[e]*Department of Chemical Technology, Recycling and Ecology, Azerbaijan Technical University, 25, H.Javid ave, Baku, Azerbaijan*
[*]*e-mail: namiqst@gmail.com, +994503225269*

Abstract. Novel imidazole-functionalized pyridinium-fused selenadiazolium salts were synthesised and structurally characterised as versatile chalcogen bond (ChB) donors. The compounds were obtained from the reaction of 2-pyridylselenyl chloride with 4,5-dicyanoimidazole, yielding a monocationic chloride salt and a dicationic perrhenate derivative. X-ray diffraction analysis revealed that both salts adopt nearly planar selenadiazole cores and T-shaped geometries stabilized by intermolecular Se···X (X = Cl, O) chalcogen bonds. In the solid state, monocationic salt forms a supramolecular polymer *via* a combination of $[Se\cdots Cl]_2$ dimerisation and, secondary, Se···N chalcogen bonds involving the imidazole moiety. Results of Hirshfeld surfaces analysis reveal that crystal packing primarily determined by intermolecular contacts involving hydrogen atoms. Theoretical QTAIM and RDG analyses confirmed the presence and attractive nature of key noncovalent interactions (Se···Cl, Se···N, Se···O, H···Cl, H···O), with estimated energies consistent with typical chalcogen and hydrogen bonds. This work illustrates a rational strategy for managing supramolecular organization through synergistic noncovalent interactions, offering a pathway toward predictable chalcogen-bond-driven architectures for crystal engineering and functional materials.

Keywords: imidazole, selenadiazolium salt, supramolecular polymer, chalcogen bond, noncovalent interactions.

Received: 06 May 2026/ Revised final: 11 June 2026/ Accepted: 12 June 2026

Introduction

Despite its significant directionality and tunable strength, chalcogen bonding (ChB) has not yet been widely employed to construct extended supramolecular architectures. In this interaction, a chalcogen atom acts as an electrophilic acceptor of electron density from a Lewis base [1-3]. This stands in contrast to the ubiquitous use of hydrogen bonding (HB), a classical and foundational tool for building supramolecular assemblies and frameworks [4-6].

Recently, novel selenadiazolium salts have emerged as promising chalcogen-bond donors [7-14]. In certain cases, these cations assemble into supramolecular Se_2N_2 squares *via* antiparallel Se···N ChB, a motif with potential for use as a structural node in extended supramolecular architectures [7-9, 15-21]. However, the formation of these squares proved inconsistent and was highly sensitive to substituents on the selenadiazolium core. Competing noncovalent interactions often dominate, disrupting square formation and dictating alternative packing modes. This observation motivated the exploration of strategies for achieving reliable, rational assembly of Se_2N_2 squares. In particular, the use of multifunctional building blocks that incorporate additional donor or acceptor sites could help steer supramolecular assembly through hierarchical or synergistic noncovalent interactions, favouring the desired ChB-driven motifs.

Imidazole is a five-membered aromatic heterocycle featuring two nitrogen atoms (one pyrrole-type NH and one pyridine-type N) that confer versatility in molecular recognition and supramolecular chemistry. Its ability to act simultaneously as a hydrogen bond donor and acceptor makes it a privileged scaffold in crystal engineering. Furthermore, the imidazole ring can participate in π–π stacking, coordinate to metal centres, and, when appropriately functionalized, engage in chalcogen and halogen bonding.

In this context, the synthesis and structural characterization of new cationic systems derived from the reaction of 2-pyridylselenyl chloride with 4,5-dicyanoimidazole is reported. The resulting compounds feature pyridinium-fused selenadiazole cores linked *via* an imidazole spacer. It was proposed that the imidazole moiety, with its dual hydrogen-bonding capability and potential for secondary ChB interactions, could act as a versatile supramolecular auxiliary. This might either reinforce the formation of classical Se_2N_2 squares or guide the assembly into novel architectures, such as one-dimensional polymers, by providing additional interaction vectors. Herein, the synthesis, X-ray structures, and theoretical investigation of new selenadiazolium salts are described, demonstrating how the imidazole unit influences the solid-state organization through a combination of Se···X (X= Cl, O) chalcogen bonds and secondary interactions, leading to the formation of a 1D supramolecular polymer in one case.

Experimental

Materials

No uncommon hazards are noted derived from the experimental work carried out. All manipulations were carried out in air. All the reagents used in this study ($PhICl_2$, 2,2′-dipyridyldiselenide, 4,5-dicyanoimidazole, NH_4ReO_4), were obtained from the commercial sources (Aldrich, TCI-Europe, Strem, ABCR). Commercially available solvents were purified by conventional methods and distilled immediately prior to use.

Instruments

The *^{1}H* and *^{13}C-NMR spectra* were measured on a Bruker Avance neo 700 spectrometer, using D_2O as the NMR solvent. Chemical shifts are indicated in parts per million (ppm) relative to tetramethylsilane as an internal standard. Coupling constants (*J*) are reported in Hertz (Hz). C, H, and N elemental analyses were carried out on a Euro EA 3028HT CHNS/O analyser.

X-ray crystal structure determination

The single-crystal X-ray diffraction data for **3** and **4** were obtained at the Collective Use Center of the Institute of General and Inorganic Chemistry of the Russian Academy of Sciences on a three-circle Bruker SMART Apex II or Bruker D8 Venture (graphite monochromator, ω and φ scanning mode). The data were indexed and integrated using the SAINT program (Bruker, SAINT, v. 8.40A, Bruker AXS Inc., Madison, WI, 2019), and then scaled and corrected for absorption using the SADABS program. For details, see Table S1 in Supplementary material.

The structures were determined by direct methods and refined by full-matrix least squares technique on F2 with anisotropic displacement parameters for non-hydrogen atoms. Hydrogen atoms are calculated from geometric considerations. All calculations were carried out using the SHELXL program and OLEX2 program package.

Level B errors in crystal **3** are due to the low crystal quality. The short Se···O contacts (level A errors in crystal **4**) correspond to intermolecular chalcogen bonds.

Crystallographic data for all investigated compounds have been deposited with the Cambridge Crystallographic Data Center, CCDC 2528228-2528229. Copies of this information may be obtained free of charge from the Director, CCDC, 12 Union Road, Cambridge CB2 1EZ, UK (Fax: +44 1223 336033; e-mail: deposit@ccdc.cam.ac.uk or www.ccdc.cam.ac.uk).

Synthesis of 3-(5-cyano-1*H*-imidazol-4-yl)-[1,2,4]selenadiazolo[4,5-a]pyridin-4-ium chloride (3).

A solution of $PhICl_2$ (18 mg, 64 μmol) in CH_2Cl_2 (2 mL) was added to a suspension of 2,2′-dipyridyldiselenide (20 mg, 64 μmol) and 4,5-dicyanoimidazole (15 mg, 128 μmol) in CH_2Cl_2 (3 mL), and the reaction mixture was left with stirring at room temperature for 12 h. After that, the solution was decanted from a colourless precipitate, and the solid was washed with acetone (3 × 1 mL), Et_2O (3 × 1 mL) and dried under vacuum. ^{1}H NMR (700 MHz, D_2O) δ 10.32 (d, J = 6.8 Hz, 1H), 8.91 (d, J = 8.7 Hz, 1H), 8.49–8.46 (m, 1H), 8.25 (s, 1H), 8.07–8.05 (m, 1H). ^{13}C NMR (176 MHz, D_2O) δ 168.5, 147.5, 140.2, 140.0, 138.1, 136.9, 125.9, 123.2, 111.0, 107.0. Elem. anal. calculated for $C_{10}H_6ClN_5Se$: C, 38.67; H, 1.95; N, 22.55. Found: C, 38.75; H, 2.21; N, 22.39. Yield: 63%.

***Synthesis of* 3,3'-(1*H*-imidazole-4,5-diyl) bis([1,2,4]selenadiazolo[4,5-a]pyridin-4-ium) perrhenate (4).**

3,3'-(1*H*-imidazole-4,5-diyl)bis([1,2,4] selenadiazolo[4,5-a]pyridin-4-ium) chloride (30 mg, 32 μmol) was dissolved in MeOH (1.5 mL) and the addition of MeOH solution (1.5 mL) of NH_4ReO_4 (200 mg, 746 μmol) resulted in the formation of a colourless crystals, which were washed with acetone (3 × 1 mL), Et_2O (3 × 1 mL) and dried under vacuum. The compound was insoluble in common deuterated solvents, which precluded NMR analyses. Elem. anal. calculated for $C_{15}H_{10}N_6O_8Re_2Se_2$: C 19.32; H, 1.08; N, 9.01. Found: C 19.58; H 1.21; N 8.78. Yield: 76%.

Computational details

Hirshfeld surfaces analysis for the X-ray structures **3** and **4** was carried out in CrystalExplorer program (version 17.5). The normalized contact distances, d_{norm}, based on Bondi's van der Waals radii, were mapped into the Hirshfeld surfaces. In the colour scale, negative values of d_{norm} are visualised by the red colour, indicating contacts shorter than the sum of vdW radii. The white colour denotes intermolecular distances close to the vdW contacts with d_{norm} equal to zero. In turn, contacts longer than the sum of vdW radii with positive d_{norm} values are coloured with blue.

The DFT calculations based on the experimental X-ray structures **3** and **4** were carried out using the dispersion-corrected hybrid functional ωB97XD with the help of Gaussian-09 program package. The Douglas–Kroll–Hess 2nd order scalar relativistic calculations requested relativistic core Hamiltonian were carried out using the DZP-DKH basis sets for all atoms. The topological analysis of the electron density distribution with the help of the atoms in molecules (QTAIM) method developed by Bader was performed by using the Multiwfn program (version 3.7). The Cartesian atomic coordinates for model supramolecular associates are presented in Table S1, Supplementary material.

Results and discussion

The synthesis of the target cationic selenadiazolium salts was achieved through a straightforward procedure utilizing 2-pyridylselenyl chloride (**1**) as a versatile selenating reagent (Scheme 1).

First, the reaction of commercially available 2,2′-dipyridyldiselenide with one equivalent of phenyliodine(III) dichloride in dichloromethane generated ambiphilic **1** *in situ*. This reagent was subsequently treated with 4,5-dicyanoimidazole. The reaction proceeded *via* the addition of **1** to one nitrile group to yield the monocationic salt **3** as a chloride. This compound was isolated in good yield (63%) as a colourless solid. To obtain a dicationic species, **2** was reacted with two equivalents of **1**, leading to the functionalization of both nitrile groups. Subsequent anion metathesis with ammonium perrhenate in methanol afforded the desired bis-selenadiazolium salt **4**, isolated as its perrhenate derivative.

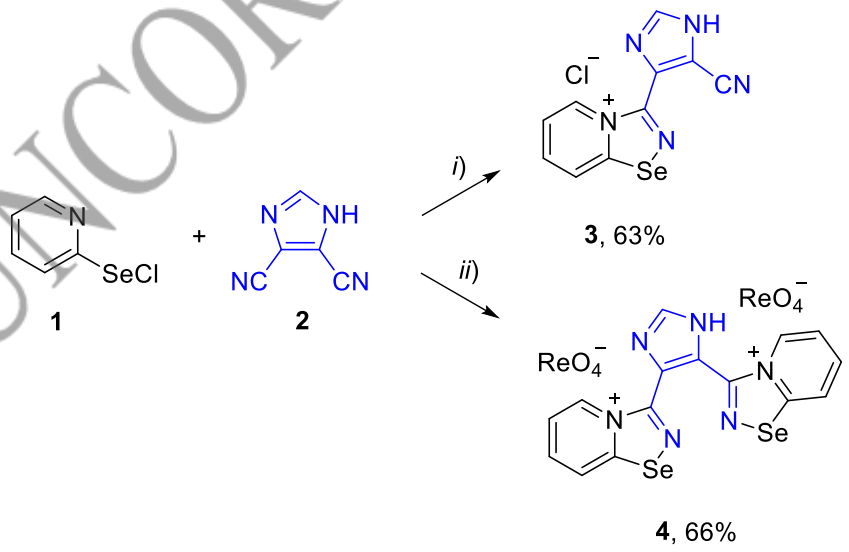

Reagents and conditions. i) 1 equiv 2-PySeCl; ii) 2 equiv 2-PySeCl, then saturated MeOH solution of NH_4ReO_4.

Scheme 1. **Reactions between 2-PySeCl and 4,5-dicyanoimidazole.**

Structural confirmation of the prepared compounds was achieved using ^{1}H, ^{13}C NMR spectroscopy, along with X-ray diffraction analysis (Figure 1). For the formed heterocyclic product **3**, ^{1}H, ^{13}C chemical shifts and coupling constants are typical of those observed for 1,2,4-selenadiazolium salts. The ^{1}H NMR spectrum displays a doublet at 10.32 ppm assigned to the pyridinium proton adjacent to the selenium atom, along with a characteristic singlet at δ 8.25 for the imidazole CH proton. The ^{13}C NMR spectrum corresponds to the expected structure. Suitable single crystals for the X-ray study were grown *via* slow evaporation of a dichloromethane solution of **3**, whereas crystals of **4** were obtained directly from the methanol reaction mixture.

Compounds **3** and **4** are bicyclic and bis-bicyclic cationic systems (Figure 1), respectively. The selenium-containing rings are nearly planar, with C_{py}–Se–N' –C torsion angles of 1.3(7)° for **3** and –0.18° for **4**. The N'–Se bond distances of 1.821(7) Å in **3** and 1.821(6)/1.833(6) Å in **4** correspond to typical single bonds, while the C=N bond lengths of 1.283(3) Å and 1.288(4) Å are characteristic of double bonds [22]. The selenium atom adopts a T-shaped geometry, supported by non-covalent Se···Cl/(ReO_4) interactions. The C_{py}–Se–N' angles are 88.7(3)° for **3** and 87.7(3)° for **4**, and the Se···Cl and Se···(ReO_4) contact distances are 2.905 Å and 2.742 Å, respectively. These structural features align with those previously reported for related selenadiazolium salts [7,11,14].

Table 1

Selected bond lengths (Å) and angles (°) for 3.

Bond	*Value*	*Bond*	*Value*
Se1–N2	1.821(7)	Se2–N7	1.828(7)
Se1–C1	1.862(9)	Se2–C11	1.832(10)
Se1–Cl1	2.985(2)	Se2–Cl2	2.908(4)
Se1···N8	3.056(8)	Se2–Cl2[1]	3.263(5)
Se1···Cl1	3.263(5)		
Angle	°	*Angle*	°
N2–Se1–C1	88.7(3)	N7–Se2–C11	87.8(4)
N2–Se1–N8	87.0(3)	N7–Se2–Cl2	173.0(3)
N2–Se1–Cl1	177.9(2)	C11–Se2–Cl2	91.6(3)
C1–Se1–N8	173.9(3)	Se2–Cl2–Se2[1]	81.60(11)
C1–Se1–Cl1	91.3(3)	Cl2–Se2–Cl2[1]	98.4(2)
Cl1–Se1–N8	92.88(15)		

[1]2-X,1-Y,2-Z

Table 2

Selected bond lengths (Å) and angles (°) for 4.

Bond	*Length*	*Angle*	*Value*
Se1–N2	1.821(6)	Re1–O2–Se2	113.3(2)
Se1[2]–O7	3.383(6)	Re1–O3–Se2[1]	104.5(2)
Se1–C1	1.857(7)	Re2–O7–Se1[2]	94.4(2)
Se1–O8	2.744(5)	Re2–O8–Se1	120.4(2)
Se2–N6	1.831(6)	N2–Se1–O8	171.8(2)
Se2–C11	1.874(7)	N2–Se1–C1	87.7(3)
Se2–O2	2.675(5)	C1–Se1–O8	86.3(2)
Se2[1]–O3	3.047(5)	N6–Se2–O2	168.2(2)
		N6–Se2–C11	87.9(3)
		C11–Se2–O2	83.6(2)

[1]2-X,-Y,-Z; [2]2-X,1-Y,1-Z

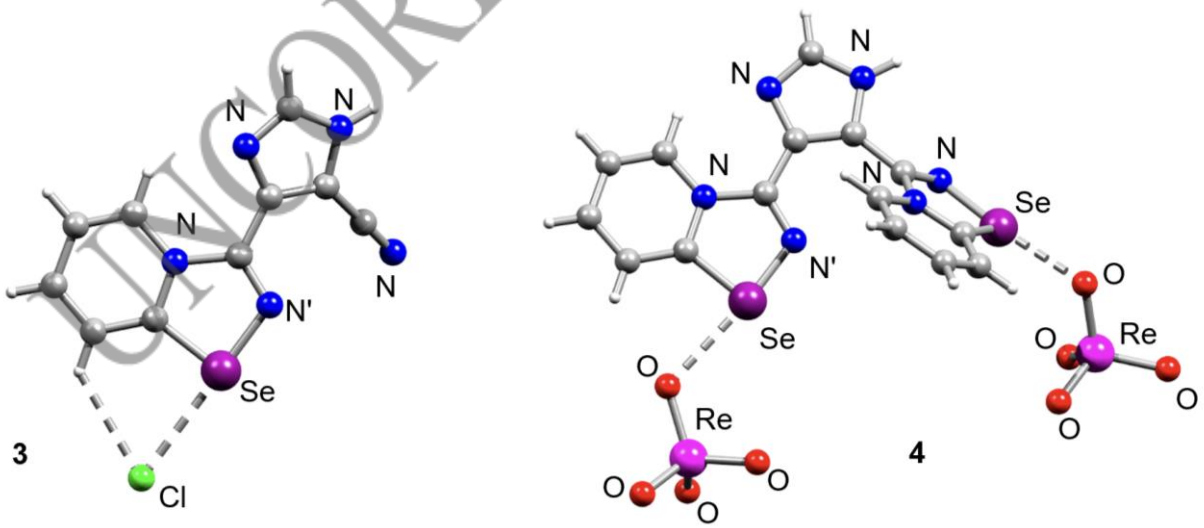

Figure 1. Ball-and-stick representation of the crystal structure of 3, and 4. Grey and light-grey spheres represent carbon and hydrogen, respectively.

In the crystal, the crystallographically independent part of the unit cell of compound **3** contains two independent cations and anions, which are linked to each other *via* a Se···N *σ*-hole interaction (Se···N = 3.057(10) Å). The second selenium atom forms a dimeric pair with a symmetrically related cation linked through an inversion centre *via* a four-centre $[Se\cdots Cl]_2$ interaction with two bridging chlorine atoms (Se···Cl distances of 2.908(4) Å and 3.263(5) Å), ultimately yielding a tetrameric molecule (Figure 2). Similar dimerization has been observed for previously described pyridinium-containing 1,2,4-selenadiazoles [8,10]. The imidazolium group of the second cation participates in the formation of CH···N hydrogen bonds, linking the tetramers into polymeric chains, which in turn are connected to each other through CH···Cl and NH···Cl hydrogen bonds (Figure 3).

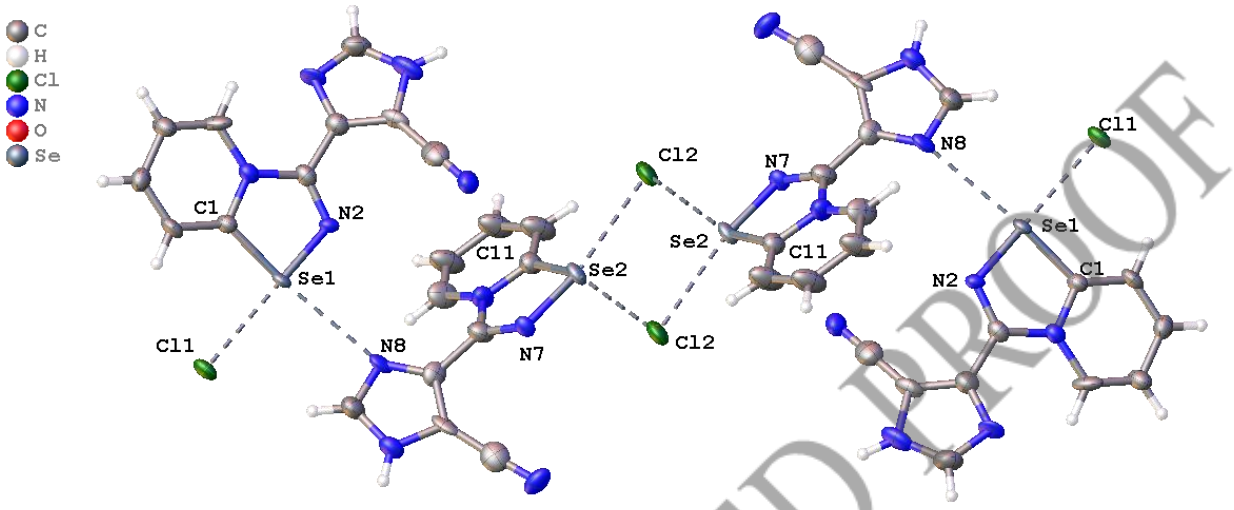

Figure 2. Ball-and-stick representation of the crystal structure of 3 demonstrating $[Se\cdots Cl]_2$, Se···N and H···Cl interactions. Grey and light-grey spheres represent carbon and hydrogen, respectively.

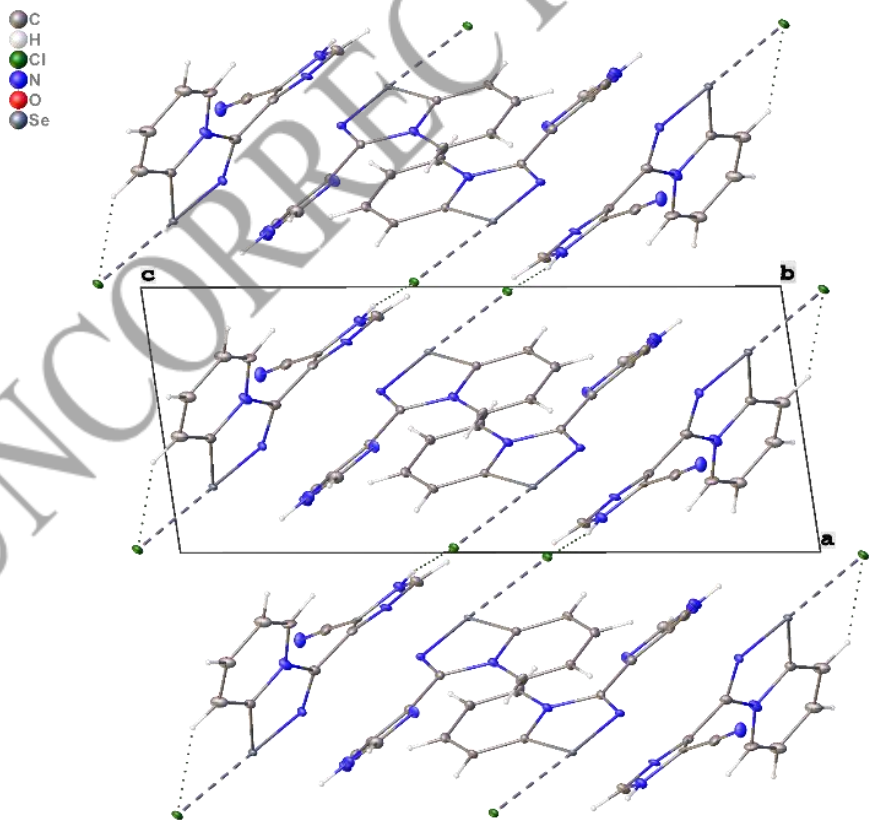

Figure 3. Packing diagram of 3 along *b*-axes.

In the crystal of compound **4**, two pairs of anions link the dications into a polymer chain oriented parallel to the crystallographic direction [011] (Figure 4).

Theoretical investigation of non-covalent interactions

To investigate the presence and characteristics of discussed non-covalent interactions in compounds **3** and **4**, we conducted DFT calculations followed by the topological analysis of the electron density distribution (QTAIM analysis) at the ωB97XD/DZP-DKH level of theory for model supramolecular associates (see Computational details and Table S1 in Supplementary material). Results of QTAIM analysis are summarized in Table 3, the contour line diagrams of the Laplacian of electron density distribution $\nabla^2\rho(\mathbf{r})$, bond paths, and selected zero-flux surfaces, visualization of electron localization function (ELF) and reduced density gradient (RDG) analyses for these non-covalent contacts are shown in Figure 5.

Values of the density of all electrons - $\rho(\mathbf{r})$, Laplacian of electron density - $\nabla^2\rho(\mathbf{r})$ and appropriate λ_2 eigenvalues, energy density – H_b, potential energy density - $V(\mathbf{r})$, Lagrangian kinetic energy - $G(\mathbf{r})$, and electron localization function - ELF (a.u.) at the bond critical points (3, –1), corresponding to non-covalent interactions in compounds **3** and **4**, and approximately estimated strength for these interactions $E_{int} = -V(\mathbf{r})/2$ (kcal/mol). * The Bondi's (shortest) van der Waals radii for H, O, N, Cl, and Se atoms are 1.20, 1.52, 1.55, 1.75, and 1.90 Å, respectively [23].

Table 3

QTAIM Parameters for Non-Covalent Interactions in the Model Associates of 3 and 4.

*Contact**	*ρ(r)*	*∇²ρ(r)*	*λ₂*	*H_b*	*V(r)*	*G(r)*	*ELF*	*E_int*
				3				
Se···Cl, 2.91 Å	0.026	0.073	-0.026	0.001	-0.016	0.017	0.125	**5.0**
Se···Cl, 2.99 Å	0.023	0.061	-0.023	0.001	-0.013	0.014	0.125	**4.1**
Se···Cl, 3.26 Å	0.013	0.038	-0.013	0.001	-0.007	0.008	0.063	**2.2**
Se···N, 3.06 Å	0.013	0.043	-0.013	0.002	-0.007	0.009	0.048	**2.2**
H···Cl, 2.67 Å	0.012	0.040	-0.012	0.002	-0.007	0.009	0.039	**2.2**
H···Cl, 2.73 Å	0.011	0.035	-0.011	0.001	-0.006	0.007	0.036	**1.9**
H···Cl, 2.86 Å	0.008	0.023	-0.008	0.001	-0.004	0.005	0.029	**1.3**
				4				
Se···O, 2.68 Å	0.024	0.086	-0.024	0.002	-0.017	0.019	0.079	**5.3**
Se···O, 2.74 Å	0.021	0.075	-0.021	0.002	-0.014	0.016	0.071	**4.4**
H···O, 2.33 Å	0.014	0.059	-0.014	0.002	-0.010	0.012	0.032	**3.1**
H···O, 2.39 Å	**0.011**	**0.048**	**-0.011**	**0.002**	**-0.008**	**0.010**	**0.024**	**2.5**

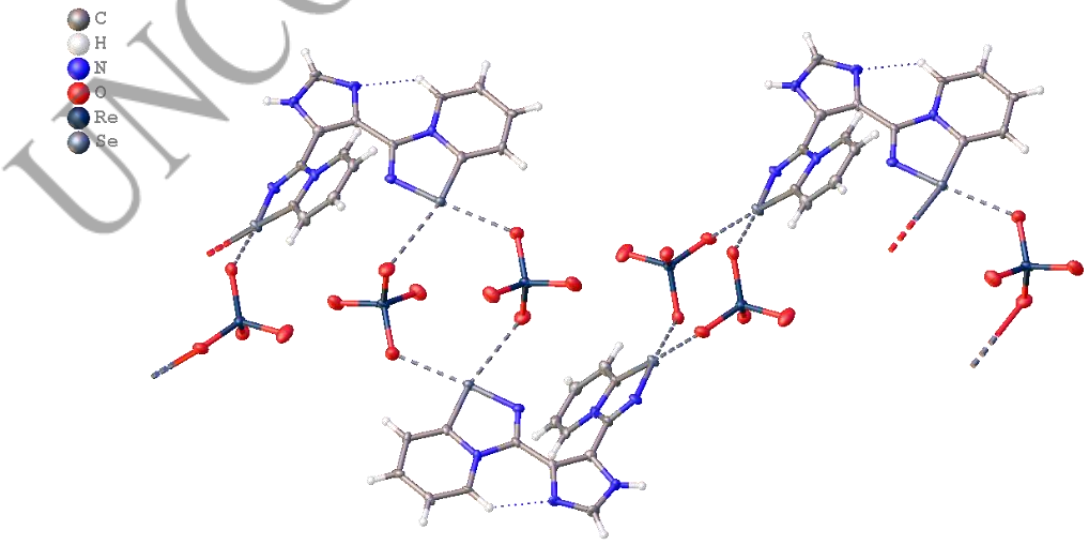

Figure 4. A fragment of the polymer chain of compound 4 formed by Se···O chalcogen bonds.

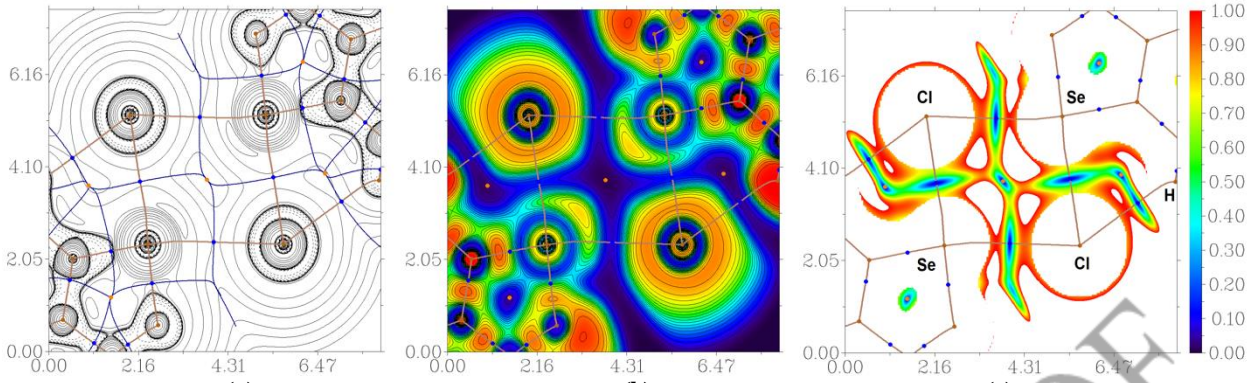

(a) *(b)* *(c)*

Figure 5. Contour line diagram of the Laplacian of electron density distribution $\nabla^2\rho(r)$, bond paths, and selected zero-flux surfaces (*a*), visualization of electron localization function (ELF) *(b)* and reduced density gradient (RDG) *(c)* analyses for non-covalent contacts $[Se\cdots Cl]_2$ and H···Cl in 3. Bond critical points (3, –1) are shown in blue, nuclear critical points (3, –3) – in pale brown, ring critical points (3, +1) – in orange, bond paths are shown as pale brown lines, length units – Å, and the colour scale for the ELF and RDG maps is presented in a.u.

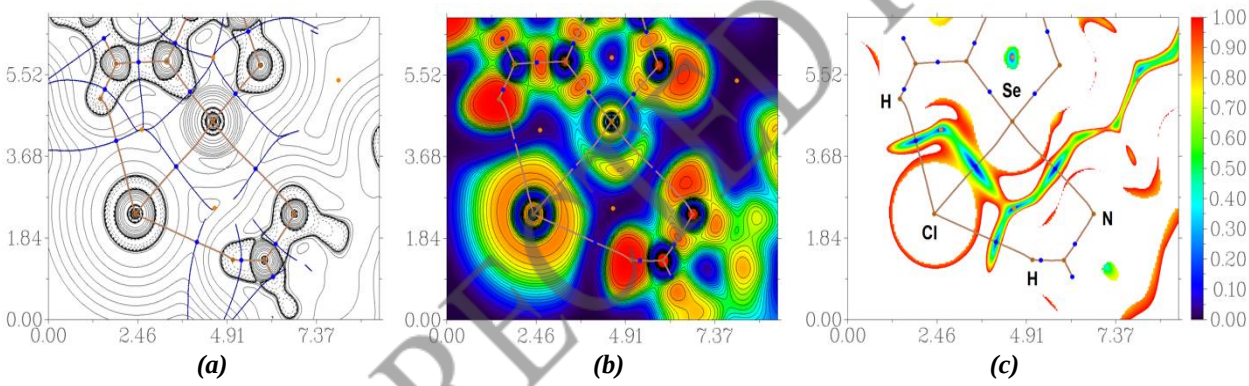

(a) *(b)* *(c)*

Figure 6. Contour line diagram of the Laplacian of electron density distribution $\nabla^2\rho(r)$, bond paths, and selected zero-flux surfaces *(a)*, visualization of electron localization function (ELF) *(b)* and reduced density gradient (RDG) *(c)* analyses for non-covalent contacts Se···Cl, Se···N, and H···Cl in 3. Bond critical points (3, –1) are shown in blue, nuclear critical points (3, –3) – in pale brown, ring critical points (3, +1) – in orange, bond paths are shown as pale brown lines, length units – Å, and the colour scale for the ELF and RDG maps is presented in a.u.

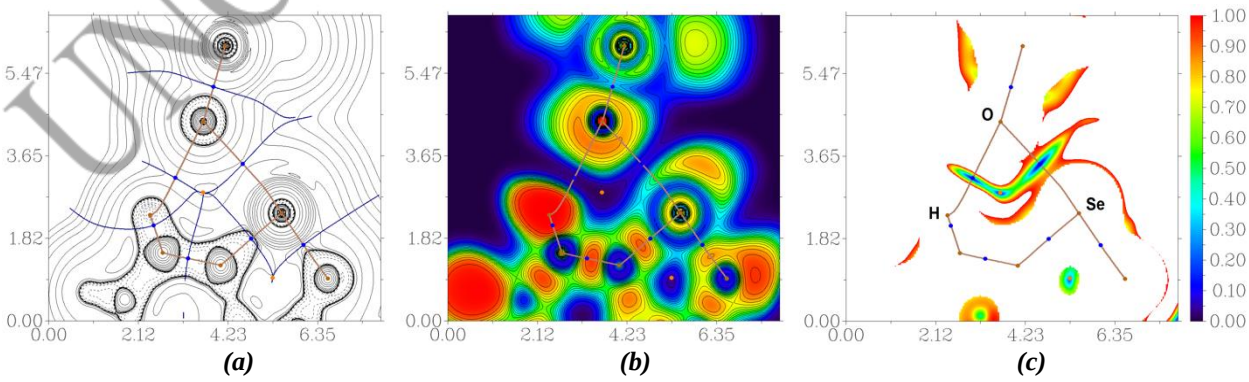

(a) *(b)* *(c)*

Figure 7. Contour line diagram of the Laplacian of electron density distribution $\nabla^2\rho(r)$, bond paths, and selected zero-flux surfaces *(a)*, visualization of electron localization function (ELF) *(b)* and reduced density gradient (RDG) *(c)* analyses for non-covalent contacts Se···O and H···O in 4. Bond critical points (3, –1) are shown in blue, nuclear critical points (3, –3) – in pale brown, ring critical points (3, +1) – in orange, bond paths are shown as pale brown lines, length units – Å, and the colour scale for the ELF and RDG maps is presented in a.u.

The QTAIM analysis of model supramolecular associates demonstrates the presence of bond critical points (3, –1) for short contacts Se···Cl, Se···N, Se···O, H···Cl, and H···O in **3** and **4** (Table 3 and Figures 5–7). The low magnitude of the electron density, positive values of the Laplacian of electron density, very close to zero and positive values of energy density, magnitudes of electron localization function in these bond critical points (3, –1) and estimated strengths for appropriate short contacts (chalcogen bonds are approximately two time stronger than hydrogen bonds in these chemical systems) are typical for such non-covalent interactions [7,9,10,24-30]. The balance $G(\mathbf{r})/V(\mathbf{r})$ in bond critical points (3, –1) reveals purely non-covalent nature of these contacts, and the sign of λ_2 allows to distinguish these interactions as bonding (attractive, $\lambda_2 < 0$) [31,32].

The Hirshfeld surface analysis was carried out for the X-ray structures **3** and **4** to understand what kind of intermolecular contacts gives the largest contributions in crystal packing**.** In the case of **3**, the Hirshfeld surface analysis reveals the following contributions of intermolecular contacts: N-H 25.1%, H-H 15.0%, C-H 12.0%, N-C 9.9%, Cl-H 6.2%, Se-C 5.6%, Se-H 4.5%, Cl-C 4.0%, Se-N 3.5%, N-N 3.3%, C-C 3.2%, O-H 2.7%, Cl-Se 1.9%, Cl-N 1.7%, O-C 0.7%, O-N 0.5%. In case of **4**, the Hirshfeld surface analysis reveals following contributions of intermolecular contacts: O-H 24.5%, H-H 15.7%, Se-O 11.7%, N-H 11.1%, O-C 9.4%, O-N 5.8%, C-H 4.9%, N-C 4.8%, C-C 3.6%, Se-H 3.2%, Se-C 3.2%, Se-N 1.0%, Se-Se 0.8%, N-N 0.4%.

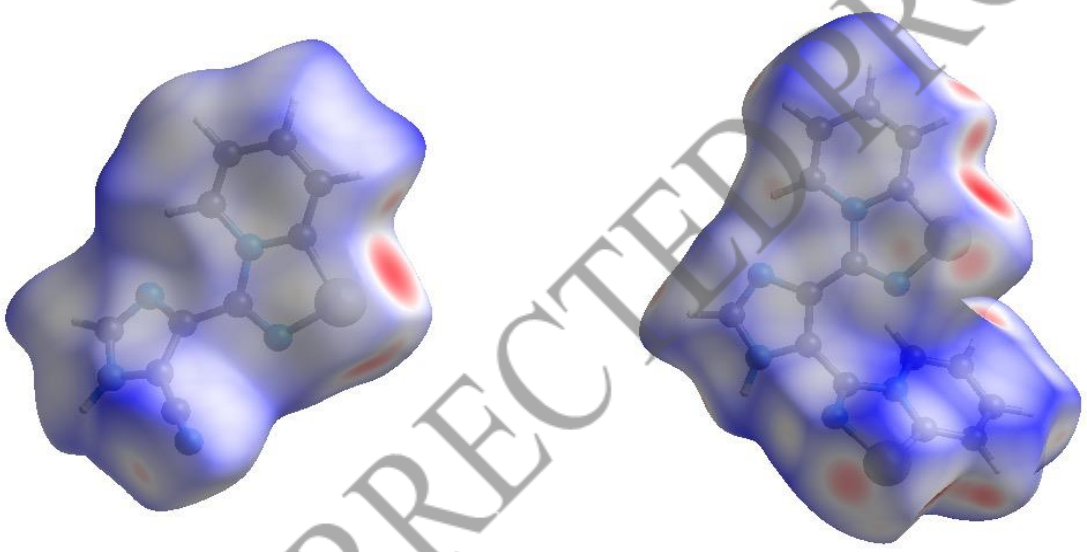

(a) ***(b)***

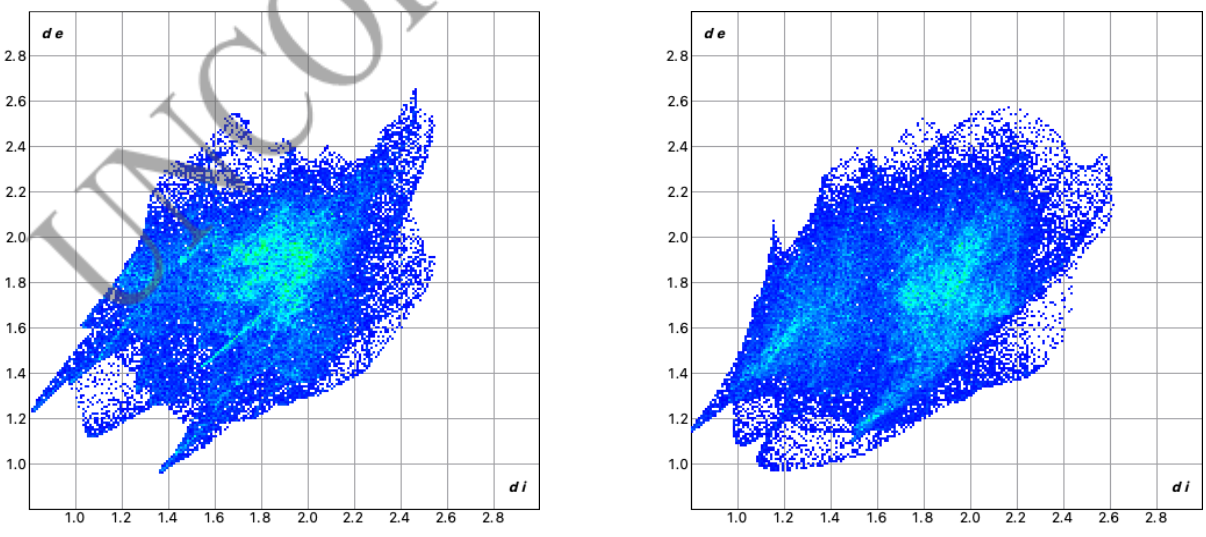

(c) ***(d)***

Figure 8. Visualization of Hirshfeld surfaces for the X-ray structures 3 *(a)* and 4 *(b)* and appropriate fingerprint plots for 3 *(c)* and 4 *(d)*.

For the visualisation of Hirshfeld surfaces, was used a mapping of the normalized contact distance (d_{norm}), its negative value enables identification of molecular regions of substantial importance for detection of short contacts, and the fingerprint plots, which are two-dimensional histograms derived from Hirshfeld surfaces, mapping the distances from each point on the surface to the nearest atom inside (d_i) and outside (d_e) the surface (Figure 8).

Thus, results of Hirshfeld surface analysis for X-ray structures **3** and **4** reveal that noncovalent intermolecular contacts involving hydrogen atoms give the largest contributions in the crystal packing in both cases.

Conclusions

In summary, two novel cationic selenadiazolium salts derived from the reaction of 2-pyridylselenyl chloride with 4,5-dicyanoimidazole were synthesized and characterized. The structural analysis revealed that both compounds exhibit nearly planar selenium-containing cycles and adopt T-shaped geometries stabilised by intramolecular Se···X (X = Cl, O) chalcogen bonds. In the solid state, the monocationic salt **3** forms a 1D supramolecular polymer *via* a combination of $[Se\cdots Cl]_2$ dimerization and Se···N chalcogen bonds involving the imidazole moiety. This demonstrates the ability of the imidazole unit to act as a versatile supramolecular auxiliary, providing additional interaction vectors that guide assembly beyond well-documented Se_2N_2 squares.

Theoretical QTAIM and RDG analyses confirmed the presence and attractive nature of key noncovalent interactions (Se···Cl, Se···N, Se···O, H···Cl, and H···O), with estimated interaction energies consistent with typical chalcogen and hydrogen bonds. The results highlight the hierarchical role of chalcogen bonding in directing solid-state organization, particularly in the presence of multifunctional building blocks.

Overall, this work illustrates a rational strategy for steering supramolecular assembly through synergistic noncovalent interactions, offering a pathway toward predictable chalcogen-bond-driven architectures with potential applications in crystal engineering and functional materials.

Funding

This work was performed with the support of the RSCF (No. 22-73-10007-П).

Supplementary information

Supplementary data are available free of charge at http://cjm.ichem.md as PDF file.

References

1. Wang, W.; Ji, B.; Zhang, Y. Chalcogen bond: A sister noncovalent bond to halogen bond. The Journal of Physical Chemistry A, 2009, 113(28), pp. 8132–8135. DOI: https://doi.org/10.1021/jp904128b
2. Pascoe, D.J.; Ling, K.B.; Cockroft, S.L. The origin of chalcogen-bonding interactions. Journal of the American Chemical Society, 2017, 139(42), pp. 15160–15167. DOI: https://doi.org/10.1021/jacs.7b08511
3. Bortoli, M.; Ahmad, S.M.; Hamlin, T.A.; Bickelhaupt, F.M.; Orian, L. Nature and strength of chalcogen–π bonds. Physical Chemistry Chemical Physics, 2018, 20(43), pp. 27592–27599. DOI: https://doi.org/10.1039/C8CP05922E
4. Liu, Y.; Wang, L.; Zhao, L.; Zhang, Y.; Li, Z.-T.; Huang, F. Multiple hydrogen bonding driven supramolecular architectures and their biomedical applications. Chemical Society Reviews, 2024, 53(3), pp. 1592–1623. DOI: https://doi.org/10.1039/D3CS00705G
5. Adachi, T.; Ward, M.D. Versatile and resilient hydrogen-bonded host frameworks. Accounts of Chemical Research, 2016, 49(12), pp. 2669–2679. DOI: https://doi.org/10.1021/acs.accounts.6b00360
6. Mohan, B.; Singh, G.; Gupta, R.K.; Sharma, P.K.; Solovev, A.A.; Pombeiro, A.J.L.; Ren, P. Hydrogen-bonded organic frameworks (HOFs): Multifunctional material on analytical monitoring. TrAC Trends in Analytical Chemistry, 2024, 170, 117436, pp. 1–17. DOI: https://doi.org/10.1016/j.trac.2023.117436
7. Khrustalev, V.N.; Grishina, M.M.; Matsulevich, Z.V.; Lukiyanova, J.M.; Borisova, G.N.; Osmanov, V.K.; Novikov, A.S.; Kirichuk, A.A.; Borisov, A.V.; Solari, E.; Tskhovrebov, A.G. Novel cationic 1,2,4-selenadiazoles: synthesis *via* addition of 2-pyridylselenyl halides to unactivated nitriles, structures and four-center Se···N contacts. Dalton Transactions, 2021, 50(31), pp. 10689–10691. DOI: https://doi.org/10.1039/d1dt01322j
8. Grudova, M.V.; Khrustalev, V.N.; Kubasov, A.S.; Strashnov, P.V.; Matsulevich, Z.V.; Lukiyanova, J.M.; Borisova, G.N.; Kritchenkov, A.S.; Grishina, M.M.; Artemjev, A.A.; Buslov, I.V.; Osmanov, V.K.; Nenajdenko, V.G.; Trung, N.Q.; Borisov, A.V.; Tskhovrebov, A.G. Adducts of 2-pyridylselenenyl halides and nitriles as novel supramolecular building blocks: Four-center Se···N chalcogen bonding versus other weak interactions. Crystal Growth & Design, 2022, 22(1), pp. 313–322. DOI: https://doi.org/10.1021/acs.cgd.1c00954
9. Buslov, I.V.; Novikov, A.S.; Khrustalev, V.N.; Grudova, M.V.; Kubasov, A.S.; Matsulevich, Z.V.; Borisov, A.V.; Lukiyanova, J.M.; Grishina, M.M.; Kirichuk, A.A.; Serebryanskaya, T.V.; Kritchenkov, A.S.; Tskhovrebov, A.G. 2-Pyridylselenenyl versus 2-pyridyltellurenyl halides: symmetrical chalcogen bonding in the solid state and reactivity towards nitriles. Symmetry, 2021, 13(12), 2350, pp. 1–11. DOI: https://doi.org/10.3390/sym13122350

10. Grudova, M.V.; Kubasov, A.S.; Khrustalev, V.N.; Novikov, A.S.; Kritchenkov, A.S.; Nenajdenko, V.G.; Borisov, A.V.; Tskhovrebov, A.G. Exploring supramolecular assembly space of cationic 1,2,4-selenodiazoles: Effect of the substituent at the carbon atom and anions. Molecules, 2022, 27(3), 1029, pp. 1–13. DOI: https://doi.org/10.3390/molecules27031029
11. Artemjev, A.A.; Novikov, A.P.; Burkin, G.M.; Sapronov, A.A.; Kubasov, A.S.; Nenajdenko, V.G.; Khrustalev, V.N.; Borisov, A.V.; Kirichuk, A.A.; Kritchenkov, A.S.; Gomila, R.M.; Frontera, A.; Tskhovrebov, A.G. Towards anion recognition and precipitation with water-soluble 1,2,4-selenodiazolium salts: Combined structural and theoretical study. International Journal of Molecular Sciences, 2022, 23(12), 6372, pp. 1–16. DOI: https://doi.org/10.3390/ijms23126372
12. Egorov, A.R.; Khubiev, O.; Rubanik, V.V.; Rubanik Jr., V.V.; Lobanov, N.N.; Savilov, S.V.; Kirichuk, A.A.; Kritchenkov, I.S.; Tskhovrebov, A.G.; Kritchenkov, A.S. The first selenium containing chitin and chitosan derivatives: Combined synthetic, catalytic and biological studies. International Journal of Biological Macromolecules, 2022, 209(B), pp. 2175–2187. DOI: https://doi.org/10.1016/j.ijbiomac.2022.04.199
13. Egorov, A.R.; Yagafarov, N.Z.; Artemjev, A.A.; Khubiev, O.; Medjbour, B.; Kozyrev, V.A.; Donovan Sikaona, N.; Tsvetkova, O.I.; Rubanik, V.V.; Rubanik Jr., V.V.; Kurliuk, A.V.; Shakola, T.V.; Lobanov, N.N.; Kritchenkov, I.S.; Tskhovrebov, A.G.; Kirichuk, A.A.; Khrustalev, V.N.; Kritchenkov, A.S. Synthesis and *in vitro* antifungal activity of selenium-containing chitin derivatives. Mendeleev Communications, 2022, 32(3), pp. 357–359. DOI: https://doi.org/10.1016/j.mencom.2022.05.022
14. Sapronov, A.A.; Artemjev, A.A.; Burkin, G.M.; Khrustalev, V.N.; Kubasov, A.S.; Nenajdenko, V.G.; Gomila, R.M.; Frontera, A.; Kritchenkov, A.S.; Tskhovrebov, A.G. Robust supramolecular dimers derived from benzylic-substituted 1,2,4-selenodiazolium salts featuring selenium···π chalcogen bonding. International Journal of Molecular Sciences, 2022, 23(23), 14973, pp. 1–12. DOI: https://doi.org/10.3390/ijms232314973
15. Artemjev, A.A.; Sapronov, A.A.; Kubasov, A.S.; Peregudov, A.S.; Egorov, A.R.; Khrustalev, V.N.; Borisov, A.V.; Matsulevich, Z.V.; Nenajdenko, V.G.; Gomila, R.M. Diverse cyclization pathways between nitriles with active α-2 methylene group and ambiphilic 2-pyridylselenyl reagents enabled by reversible covalent bonding. International Journal of Molecular Sciences, 2024, 25(23), 12798, pp. 1–17. DOI: https://doi.org/10.3390/ijms252312798
16. Sapronov, A.A.; Kubasov, A.S.; Khrustalev, V.N.; Artemjev, A.A.; Burkin, G.M.; Dukhnovsky, E.A.; Chizhov, A.O.; Kritchenkov, A.S.; Gomila, R.M.; Frontera, A. Se···π chalcogen bonding in 1,2,4-selenodiazolium tetraphenylborate complexes. Symmetry, 2023, 15(1), 212, pp. 1–8. DOI: https://doi.org/10.3390/sym15010212
17. Repina, O.V.; Kubasov, A.S.; Vologzhanina, A.V.; Borisov, A.V.; Kritchenkov, I.S.; Voroshilkina, K.M.; Nazarov, A.A.; Shchevnikov, D.M.; Grudova, M.V.; Gomila, R.M. Au^{III} acyclic (amino)(N-pyridinium)carbenoids: Synthesis *via* addition of 2-PySeCl to Au^{I}-bound isonitriles, structures, and cytotoxicity. International Journal of Molecular Sciences, 2025, 26(2), 483, pp. 1–12. DOI: https://doi.org/10.3390/ijms26020483
18. Sapronov, A.A.; Khrustalev, V.N.; Chusova, O.G.; Kubasov, A.S.; Kritchenkov, A.S.; Nenajdenko, V.G.; Gomila, R.M.; Frontera, A.; Tskhovrebov, A.G. Introducing cationic selenium-containing triazapentadiene ligand framework: Synthesis, coordination chemistry, and antifungal activity. Inorganic Chemistry, 2024, 63(30), pp. 13924–13937. DOI: https://doi.org/10.1021/acs.inorgchem.4c01188
19. Dukhnovsky, E.A.; Novikov, A.S.; Kubasov, A.S.; Borisov, A.V.; Sikaona, N.D.; Kirichuk, A.A.; Khrustalev, V.N.; Kritchenkov, A.S.; Tskhovrebov, A.G. Halogen bond-assisted supramolecular dimerization of pyridinium-fused 1,2,4-selenadiazoles *via* four-center Se_2N_2 chalcogen bonding. International Journal of Molecular Sciences, 2024, 25(7), 3972, pp. 1–16. DOI: https://doi.org/10.3390/ijms25073972
20. Kazakova, A.A.; Kubasov, A.S.; Chizhov, A.O.; Novikov, A.P.; Volkov, M.A.; Borisov, A.V.; Nenajdenko, V.G.; Dukhnovsky, E.A.; Bely, A.E.; Grishina, M.M. Perrhenate and pertechnetate complexes of dicationic pyridinium-fused 1,2,4-selenodiazoles featuring Se···O chalcogen bonding and anion···anion interactions. Inorganica Chimica Acta, 2024, 563, 121929, pp. 1–9. DOI: https://doi.org/10.1016/j.ica.2024.121929
21. Artemjev, A.A.; Kubasov, A.S.; Zaytsev, V.P.; Borisov, A.V.; Kritchenkov, A.S.; Nenajdenko, V.G.; Gomila, R.M.; Frontera, A.; Tskhovrebov, A.G. Novel chalcogen bond donors derived from [3+2] cycloaddition reaction between 2-pyridylselenyl reagents and isocyanates: Synthesis, structures and theoretical studies. Crystal Growth & Design, 2023, 23(4), pp. 2018–2023. DOI: https://doi.org/10.1021/acs.cgd.3c00101
22. Allen, F.H.; Kennard, O.; Watson, D.G.; Brammer, L.; Orpen, A.G.; Taylor, R. Tables of bond lengths determined by X-ray and neutron diffraction. Part 1. Bond lengths in organic compounds. Journal of the Chemical Society, Perkin Transactions 2, 1987, (12), pp. S1–S19. DOI: https://doi.org/10.1039/p298700000s1
23. Bondi, A. Van der Waals volumes and radii of metals in covalent compounds. The Journal of Physical Chemistry, 1966, 70(9), pp. 3006–3007. DOI: https://doi.org/10.1021/j100881a503
24. Mikherdov, A.; Novikov, A.; Kinzhalov, M.; Zolotarev, A.; Boyarskiy, V. Intra-/Intermolecular bifurcated chalcogen bonding in crystal structure of

thiazole/thiadiazole derived binuclear (diaminocarbene)Pd^{II} complexes. Crystals, 2 018, 8(3), 112, pp. 1–15.
DOI: https://doi.org/10.3390/cryst8030112

25. Novikov, A.S.; Gushchin, A.L. Trinuclear molybdenum clusters with sulfide bridges as potential anionic receptors *via* chalcogen bonding. CrystEngComm, 2021, 23(26), pp. 4607–4614. DOI: https://doi.org/10.1039/D1CE00514F
26. Korobeynikov, N.A.; Usoltsev, A.N.; Novikov, A.S.; Abramov, P.A.; Sokolov, M.N.; Adonin, S.A. Selenium(IV) polybromide complexes: Structural diversity driven by halogen and chalcogen bonding. Molecules, 2022, 27(16), 5355.
DOI: https://doi.org/10.3390/molecules27165355
27. Ivanov, D.M.; Baykov, S.V.; Novikov, A.S.; Romanenko, G.; Bokach, N.A.; Evarestov, R.A.; Kukushkin, V.Yu. Noncovalent sulfoxide-nitrile coupling involving four-center heteroleptic dipole–dipole interactions between the sulfinyl and nitrile groups. Crystal Growth and Design, 2020, 20(5), pp. 3417–3428.
DOI: https://doi.org/10.1021/acs.cgd.0c00196
28. Mikherdov, A.S.; Kinzhalov, M.A.; Novikov, A.S.; Boyarskiy, V.P.; Boyarskaya, I.A.; Dar'in, D.V.; Starova, G.L.; Kukushkin, V.Yu. Difference in energy between two distinct types of chalcogen bonds drives regioisomerization of binuclear (diaminocarbene)Pd^{II} complexes. Journal of the American Chemical Society, 2016, 138(42), pp. 14129–14137.
DOI: https://doi.org/10.1021/jacs.6b09133
29. Nenajdenko, V.G.; Kazakova, A.A.; Novikov, A.S.; Shikhaliyev, N.G.; Maharramov, A.M.; Qajar, A.M.; Atakishiyeva, G.T.; Niyazova, A.A.; Khrustalev, V.N.; Shastin, A.V. Copper-catalyzed reaction of N-monosubstituted hydrazones with CBr_4: Unexpected fragmentation and mechanistic study. Catalysts, 2023, 13(8), 1194, pp. 1–12.
DOI: https://doi.org/10.3390/catal13081194
30. Tskhovrebov, A.G.; Novikov, A.S.; Tupertsev, B.S.; Nazarov, A.A.; Antonets, A.A.; Astafiev, A.A.; Kritchenkov, A.S.; Kubasov, A.S.; Nenajdenko, V.G.; Khrustalev, V.N. Azoimidazole gold(III) complexes: Synthesis, structural characterization and self-assembly in the solid state. Inorganica Chimica Acta, 2021, 522, 120373, pp. 1–7.
DOI: https://doi.org/10.1016/j.ica.2021.120373
31. Contreras-García, J.; Johnson, E.R.; Keinan, S.; Chaudret, R.; Piquemal, J.-P.; Beratan, D.N.; Yang, W. NCIPLOT: A program for plotting noncovalent interaction regions. Journal of Chemical Theory and Computation, 2011, 7(3), pp. 625–632.
DOI: https://doi.org/10.1021/ct100641a
32. Johnson, E.R.; Keinan, S.; Mori-Sánchez, P.; Contreras-García, J.; Cohen, A.J.; Yang, W. Revealing noncovalent interactions. Journal of the American Chemical Society, 2010, 132(18), pp. 6498–6506.
DOI: https://doi.org/10.1021/ja100936w